EARTH SURFACE PROCESSES AND LANDFORMS, VOL. 13, 305–320 (1988)

A CONTOUR-BASED TOPOGRAPHIC MODEL FOR HYDROLOGICAL AND ECOLOGICAL APPLICATIONS

I. D. MOORE
Dept. Agricultural Engineering, University of Minnesota, St. Paul, Minnesota, U.S.A. 55108
AND
E. M. O'LOUGHLIN AND G. J. BURCH
Division of Water and Land Resources, CSIRO, Canberra, Australia 2601

Received 3 October 1986
Revised 27 April 1987

ABSTRACT

A digital model for discretizing three-dimensional terrain into small irregularly shaped polygons or elements based on contour lines and their orthogonals is described. From this subdivision the model estimates a number of topographic attributes for each element including the total upslope contributing area, element area, slope, and aspect. This form of discretization of a catchment produces natural units for problems involving water flow as either a surface or subsurface flow phenomenon. The model therefore has wide potential application for representing the three-dimensionality of natural terrain and water flow processes in the fields of hydrology, sedimentology, and geomorphology. Three example applications are presented and discussed. They are the prediction of zones of surface saturation, the prediction of the distribution of potential daily solar radiation, and the prediction of zones of erosion and deposition in a catchment.

KEY WORDS Three-dimensional Digital terrain models Water flow Saturation zones Solar radiation Erosion Deposition

INTRODUCTION

Computer based modelling of the hydrology, sedimentology, and geomorphology of real three-dimensional catchments requires overland flow and/or subsurface flow, which are the prime mechanisms for solute and sediment transport, to be modelled throughout the catchment. The topographic variables required to model these phenomena include: (1) upslope contributing area; (2) local slope of the potentiometric surface (which can often be approximated by the slope of the land surface); and (3) local aspect (which together with the local slope determines the potential solar radiation received by any point on a catchment, and hence potential evapotranspiration and snowmelt). As these variables can vary greatly over a catchment, it is important that estimates of them be obtained at locations and at scales that can reflect both the local and integrated effects of topography on runoff generation and catchment soil water status.

Digital terrain or digital elevation models (DTMs or DEMs) are the most common methods used for automatically extracting these topographic variables from raster elevation data. Manual methods of extraction, such as that used by Beven and Kirkby (1979), are time consuming and intractable on all but relatively simple catchments. Band (1986) and O'Callaghan and Mark (1984) describe the application of DEMs for determining drainage divides and stream networks. However, their discretization of catchments is too coarse for detailed modelling of runoff processes in many applications.

The most widely used data structures for DTMs and DEMs consist of grid networks. For example, the methods of determining shape and aspect developed by Sharpnack and Akin (1969) and Travis *et al.* (1975),

0197-9337/88/040305-16$08.00

and Clerici's (1980) and Mulla's (1986) method of deriving slope maps are based on grid cells. Heerdegen and Beran (1982) fitted five-parameter polynomials to grid elevation data derived from contour maps to compute both horizontal and vertical curvature characteristics of catchments. Armstrong (1976), Ahnert (1976) and Hirano (1976) used grid networks for determining and inputting the topographic variables into their simple three-dimensional slope models of landform development that included submodels of the overland flow process. The ANSWERS model (Beasley *et al.*, 1980) is one of the few hydrology/erosion/water quality models capable of representing the three-dimensionality of landscapes, but it too is based on a grid network. Most grid cell methods developed to date for hydrologic application have been too simplistic, even when used at very fine scales. Their principal drawbacks are that: (1) they do not allow water flow from one cell to be split, leading to significant error in divergent areas; and (2) the directions of flow trajectories are matched only crudely by transitions from one grid cell to another, even in very simple planar regions.

Mark (1978) noted that grid structures for spatially partitioning topographic data are not appropriate for many geomorphological applications, and in particular for digital terrain modelling. He stated that 'the chief source of this structure should be the phenomena in question, and not problems, data, or machine considerations, as is often the case'. Natural units into which a catchment should be subdivided to represent the phenomenon of waterflow are polygons formed by equipotential lines and their orthogonals, streamlines. For many water-flow processes occurring on three-dimensional catchments these can be approximated by contour lines and their orthogonals (flow trajectories) that define the boundaries of upslope drainage areas. The disadvantage of this approach is that one needs at least an order of magnitude more points in contour line form than in regular grid form to adequately describe an elevation surface. Also, it is computationally slower than the grid cell approach.

This paper describes a contour-based model that partitions three-dimensional catchments into natural units consisting of irregularly shaped polygons and estimates upslope contributing area, slope, and aspect for each unit. The distributed topographic variables calculated by the model have been used in several applications which include the identification of zones of saturation (O'Loughlin, 1986) and zones of erosion and deposition (Moore and Burch, 1986b) and the estimation of potential daily solar radiation in real three-dimensional catchments. Examples of these applications are presented.

MODEL DESCRIPTION

An idealized topographic map of a small catchment is presented in Figure 1. The model was designed to calculate, for each section of a contour (an example of which is the section defined by the line joining $j, j+1$ in Figure 1), the upslope trajectories or streamlines from the segment end-points to high point(s) on the catchment boundary (j, 0 and $j+1$, 0 in Figure 1). For each section of contour the following topographic attributes are estimated: (1) the total upslope contributing area, A_j, bounded by the contour section $j, j+1$ and the pair of adjacent trajectories, j, 0 and $j+1$, 0; (2) the area of the contour element bounded by adjacent contours and adjacent trajectories, A_{rj} (e.g. polygon defined by the points i, $i+1$, $j+1$, j in Figure 1); (3) the widths of the contour sections defining A_{rj} (b_j and b_i in Figure 1); (4) the average local slope orthogonal to the contour along each contour segment (i.e. at P_j and Q_j in Figure 1); and (5) the x, y, z coordinates of P_j and R_j (which is the centroid of the element defining A_{rj}) in Figure 1.

The model approximates contours by short straight line segments and trajectories between adjacent contours as straight lines. These approximations were made to simplify the model so that no iterative techniques were used in determining the trajectories, thus reducing the computer processing time, and to minimize storage requirements for arrays. These approximations cause little error in the estimation of the trajectories when contours are close together, but can produce substantial error when they are not. This model has evolved from a topographic model originally developed by O'Loughlin (in press).

The model calculations are performed in two programs; PREPROC and TOPO. PREPROC preprocesses the input digitized contour information, while TOPO is the program in which the trajectories and topographic attributes, described above, are calculated. Each of these programs is briefly described below.

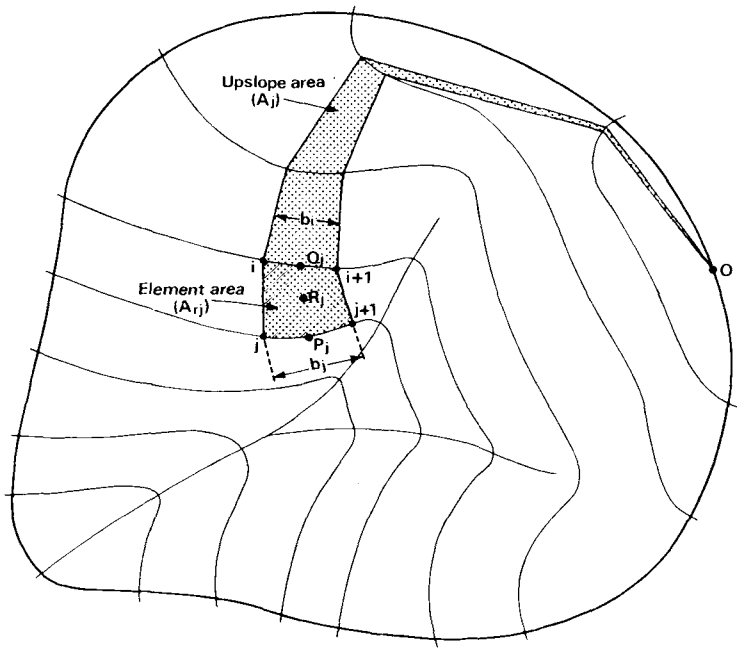

Figure 1. Idealized topographic map of a catchment showing two adjacent trajectories originating from a contour (at j and $j+1$) and the contour element they define (element with vertices at j, $j+1$, $i+1$, i)

Model inputs

The model requires sets of x, y coordinates for each contour of elevation z, the x, y, z coordinates of all high points on the catchment boundary, and the x, y coordinates of points defining the catchment boundary. It can accept up to 1500 sets of x, y coordinates for each contour line, up to 80 contour lines, up to 10 high points (on the catchment boundary), and up to 40 points defining the catchment boundary. These limits can be increased by modifying the dimension statements in the program. Any high points on the catchment boundary must also be included within the 40 sets of boundary points. The boundary points are input into the model in program TOPO.

The contour and high point data for input into the model can be generated in two ways; either by digitizing an existing topographic map, or by applying a DEM to generate contours in digital form from a regular grid of raster elevation data. If a topographic map of the catchment is already available then each contour on the map can be sequentially digitized using a flat-bed digitizer, beginning with the contour of lowest elevation. First, two points on a reference baseline of known azimuth are digitized. These are used to transform the raw digitized coordinate pairs (x, y coordinates) into a set of true eastings and northings. Second, the elevation of each contour is keyed-in (e.g. CON40, for a contour of elevation 40 m) and the contour is then digitized, producing a string of up to 1500 sets of irregularly spaced coordinates for each contour. A high point is input by keying-in the prefix HPT, followed by its elevation and then digitizing the (x, y) coordinates of the point. A high point is entered into the input file immediately after digitizing the contour segment above which it lies.

If the elevation data are in the form of randomly distributed x, y, z coordinates then a DEM consisting of a regular grid of elevations can be fitted to these data. Digital contours and high point data for input to the model can then be calculated from this regular grid. The authors have used programs developed by Hutchinson (1981, 1984) to do this.

Program PREPROC

Program PREPROC is a preprocessing program that transforms the raw digitized x, y coordinates and high points into a form that allows the topographic analysis to be performed. The raw coordinates and high points

are transformed into a set of true eastings and northings and rescaled to lie within the bounds of 0 to 1000 in both the x and y directions. If the raw coordinates were generated by digitizing a topographic map then they would be irregularly spaced along a contour. The program linearly interpolates a new string of regularly spaced x, y coordinates defining each contour. The interpolation interval is determined by the user input parameter RINT. The results of such an interpolation is demonstrated in Figure 2, which is an enlarged segment of a contour. In this figure the original rescaled coordinates defining the contour are shown as solid circles and the interpolated points are the open circles.

Users have the option of smoothing abrupt irregularities in the contours by passing the coordinates through a two-pass moving average filter as well as the option of plotting the contours. An example of this plotted output is presented in Figure 3.

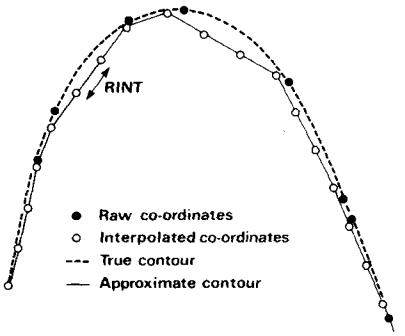

Figure 2. Linear interpolation of raw data points to a fixed spacing (RINT) along a contour line

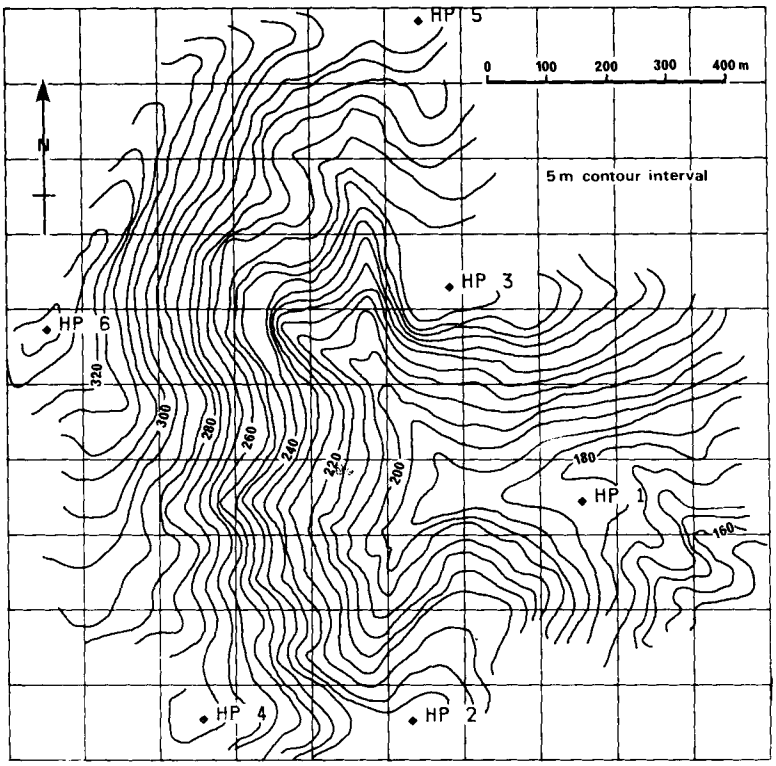

Figure 3. An example of the computer generated output from program PREPROC (with grid overlay option) showing the six high points (HP) which formed part of the digitized input to the model

The x, y coordinates of all points defining the contours are stored as two contiguous coordinate vectors (one for the x and the other for the y coordinates), beginning with the first point on the lowest contour and ending with the last point on the highest contour. The location of the first point on each contour within these vectors is also stored in vector form. If one or more gaps (greater than a specified size and where a boundary intersects the contour at two or more points) occur in a contour line then it is divided into a number of contour segments and the location of the first point of each segment and the number of segments for each contour are stored in two vectors. This method of storing the contour information permits rapid and efficient retrieval of data during the execution of program TOPO.

Program TOPO

The trajectories and topographic attributes of a catchment are computed in program TOPO. The catchment boundaries are input as up to 40 sets of x, y coordinates joined by straight line segments (see Figure 4). All contour points lying outside the catchment's boundary are excluded from the calculations. These points are determined using Hall's (1975) point in polygon routine by taking the signed summation of the angles subtended at the given point by each segment of the closed catchment boundary. If the angles sum to $\pm 360°$ then the point is inside the boundary, and if they sum to 0° then the point is outside the boundary. Using this test the first and last points on each contour segment lying on or within the catchment's boundary are identified.

Contours are digitized in a consistent direction so that model calculations proceed in the same direction for all contours. The model takes the first point on each contour segment lying on or within the boundary and identifies this as the first trajectory start point. As the calculations proceed each contour segment is divided into small sections of length b_j (see Figure 1), determined by the user input parameter PINT, thus identifying the

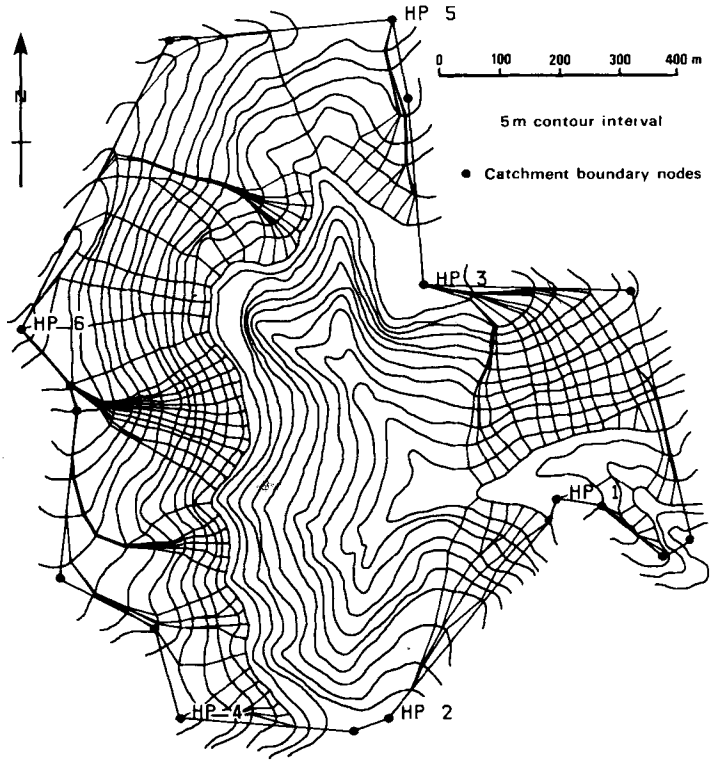

Figure 4. An example of the computer generated output from program TOPO showing the high points (HP) and the catchment boundary nodes (solid circles). The computed upslope trajectories originating from only three contour lines are shown for simplicity

coordinates of the starting points for all trajectory calculations (e.g. the points j and $j+1$ in Figure 1). PINT is a multiple of RINT (input in program PREPROC) and good results have been obtained by the authors when PINT/RINT > 10. The x, y coordinates of the mid-point of the section, P_j (see Figure 1), are also calculated.

In Figure 1 subscripts j and $j+1$ etc., refer to a given contour line for which the topographic attributes are being estimated and i and $i+1$ etc., refer to its upslope contour. The points Q_j and P_j are the points midway between j and $j+1$, and i and $i+1$, respectively, whereas R_j is the point defining the centroid of the elemental area A_{rj}. Each trajectory point is also a contour point and its address within the vectors containing the x, y coordinates of the contours is determined by the program. The points on the contour were interpolated to a regular spacing (RINT) in program PREPROC, so that b_i, the distance along the uphill contour between adjacent trajectories, is RINT times the difference between the addresses of the trajectory points i and $i+1$.

Linsley *et al.* (1949) define the aspect of a slope as 'the compass direction normal to the slope contour and pointing downslope'. In the model the aspect of the jth section of the contour (i.e. at P_j) is estimated by the orthogonal to the direction of the straight line connecting the point j to the point $j+1$ (approximately the tangent of the contour line at P_j), in the downslope direction. It is initially computed as an angle (0 to 2π radians) anticlockwise from east, and is then adjusted to give a true azimuth (clockwise from north).

Upslope trajectories from a point are computed using two criteria: minimum distance, or orthogonals. The two criteria are used in an attempt to overcome the error caused by using straight line segments between adjacent contours to define the streamlines or trajectories. The error increases as the contour lines get further apart. The application of the two criteria is determined based on the curvature of the contour line, and is controlled by a user-input parameter. The minimum distance criterion uses the minimum distance between adjacent contours to define trajectories and is applied to ridge areas where downslope flow diverges. In valleys and where flow converges trajectories are estimated by computing the orthogonal to the point of interest and projecting it to the upslope contour. In practice trajectories are streamlines that are always orthogonal to equipotential lines. A contour line is a line of equal potential energy for most terrain analyses. However, for most surface and subsurface water flow phenomena this is an approximation because the energy grade line in the downslope direction is not necessarily parallel to the land surface.

The technique for determining the orthogonal to the jth trajectory start point (see Figure 1) is similar to that described above for computing the aspect at P_j. The differences are that the orthogonal is in the upslope direction and the points $j \pm b_j/2$ are used to compute the approximate direction of the tangent to the contour at j.

Calculations for the jth trajectory (see Figure 1) begin at the trajectory start point, j. The direction of the orthogonal to j is calculated and then the string of points on the uphill contour within a user determined maximum distance from j are examined. The distance and direction (0 to 2π radians) between j and each point are computed. Points satisfying the two criteria are then selected by the model. If no point satisfying the orthogonal criterion is found, then the point determined by the minimum distance criterion is used. The curvature test is then applied and the correct uphill trajectory point is selected (i in Figure 1). The procedure is repeated for successive trajectory points until a high point or ridge, defined as the highest contour (if no high point exists), is reached. An example of trajectories computed by the model for three different contour lines of the catchment shown in Figure 3 is presented in Figure 4.

The model computes two average slope terms for each elemental area, $S1$ and $S2$ (m m^{-1}), in which

$$S1 = \left(\frac{\Delta h}{\sqrt{(x_i - x_j)^2 + (y_i - y_j)^2}} + \frac{\Delta h}{\sqrt{(x_{i+1} - x_{j+1})^2 + (y_{i+1} - y_{j+1})^2}} \right) \Big/ 2 \tag{1}$$

and

$$S2 = \left(\frac{\Delta h}{\sqrt{(x_{i+1/2} - x_{j+1/2})^2 + (y_{i+1/2} - y_{j+1/2})^2}} \right) \tag{2}$$

where Δh is the contour interval, $S1$ is the average slope of two adjacent trajectories between a contour section and its first upslope contour, and $S2$ is the average slope between P_j and Q_j. On planar slopes and in ridge areas $S1 = S2$, but if the elemental area straddles a valley $S1 \neq S2$. In such cases $S1$ is an approximation of the slope

of the land draining to a perennial or intermittent waterway, while $S2$ approximates the slope of the waterway itself. The model also estimates the average slope of the catchment between Q_j and the first contour above Q_j, adopting the same method used to calculate $S2$.

The final topographic attributes calculated by the model in program TOPO are the two area terms A_{rj}, the area of the contour element bounded by adjacent contours and adjacent trajectories, and A_j, the upslope contributing area (see Figure 1). The area enclosed by a polygon with n vertices at (x_k, y_k) is:

$$A = \left(\sum_{k=1}^{n-1} (x_{k+1} - x_k)(y_{k+1} + y_k)/2 \right) + (x_1 - x_n)(y_1 + y_n)/2 \tag{3}$$

A_{rj} and A_j are calculated by applying equation (3) to the points making up the boundaries of the two areas. If the two adjacent trajectories defining A_j terminate at two different high points then the (x_k, y_k) points defining the area must also include the nodes along the catchment boundary between the high points. It is for this reason that high points must also be catchment boundary nodes. The present version of the model can not handle high points that lie within the catchment's boundary, although work is underway to overcome this limitation.

Model results

The Geebung Creek catchment is used here to demonstrate the ability of the model to predict distributed topographic attributes of a catchment and is also used in the example applications that follow.

The catchment is 79·6 ha in area and is located about 30 km inland from the southeast coast of New South Wales, Australia, in the 51 300 ha Yambulla State Forest (37°18′S and 149°40′E). It has an easterly aspect (90°) and a relief of about 174 m. Soils are coarse textured and are generally less than one metre deep in upslope areas. They are somewhat deeper in lower-slope areas and many rock outcroppings occur throughout the catchment. The soils are highly to very highly erodible and have a low nutrient status. The vegetation consists of dry sclerophyll forest having a tall open structure. The understorey is generally sparse except for localized moderately dense stands of *Casuarina littoralis* on ridges and dense thickets of *Melaleuca squarrosa*, *Banksia serrata* and associated species and a variety of grasses around drainage lines and other wet zones (Mackay and Cornish, 1982; Moore *et al.*, 1986). Average annual rainfall is in excess of 900 mm per annum. Details of the rainfall-runoff response of the catchment are given by Moore *et al.* (1986).

A 1:5000 scale, 5 m contour interval, topographic map of the catchment (see Figure 3) produced from aerial photographs, was digitized and formed the primary input to the model. During the digitizing process six high-points were identified, as shown in Figure 3. Eighteen coordinate pairs defining the catchment's boundary (see Figure 4) were input during the execution of program TOPO. The model divided the contours into a total of 1409 sections, each 25·4 m long (i.e. PINT = 20 computer units = 25·4 m and RINT = 2 computer units = 2·54 m), and thus calculated 1409 sets of topographic attributes distributed throughout the catchment.

Three-dimensional projections of the catchment overlaid with each of the three computed topographic attributes are presented in Figures 5, 6 and 7. These projections were produced by UNIRAS, a set of FORTRAN programs for generating computer graphics. UNIRAS generates a three-dimensional surface with an overlay of colours (or a grey scale) that can be chosen to represent the variation of a location dependent function (in this case one of the three topographic attributes). The software interpolates the topographic data $(x, y, z$ data) to a regular grid and calculates smoothed values of the function over the same region.

Figure 5 shows the contributing area (in hectares) above each 25.4 m long contour segment and increasingly darker shadings reflect increasingly larger contributing areas. As expected, the smallest contributing areas are located on ridges (where flow diverges) and topslope sections of the catchment and the largest areas are in the valleys and drainage lines (where flow converges). The drainage lines are readily identifiable in this figure as the regions with darker shadings. The relationship between stream order and contributing area for the Geebung Creek catchment is also readily discernible from Figure 5. First-order streams (or drainage lines) have contributing areas of 1–5 ha and 2nd- order streams seem to form when the contributing area is about 10 ha. Although not shown in this figure, the analysis indicated that the 3rd-order stream is formed when its contributing area exceeds about 50 ha.

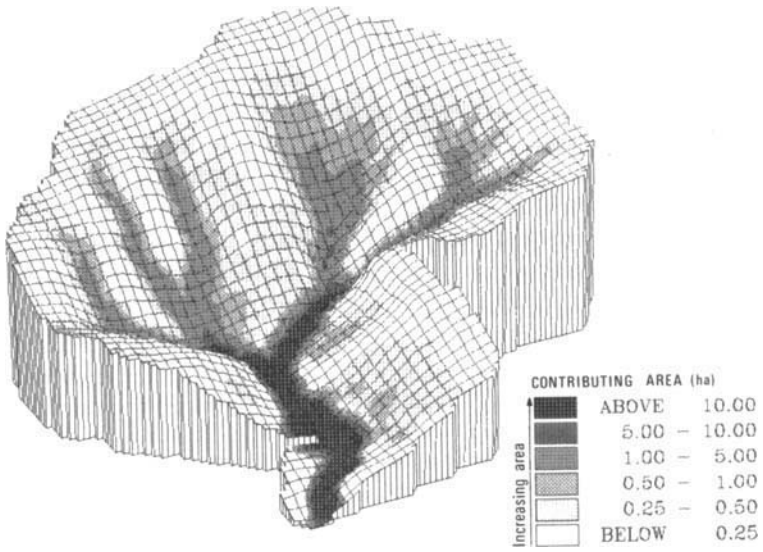

Figure 5. Distribution of upslope contributing area classes (in hectares) computed by the topographic model for the 79·6 ha Geebung Creek catchment

The Geebung Creek catchment is quite steep, exceeding 40 per cent in some parts, and this is reflected in the large relief of 174 m. The distribution of the various slope classes, computed as $S1$ using equation (2) (with slope in per cent), is shown in Figure 6. The flattest slopes, shown by the lighter shadings, occur on the ridge tops in the upland sections of the catchment and along the valley floor, upslope from the catchment outlet. The steepest slopes, corresponding to the darker shadings, tend to occur in midslope positions between ridges and drainage lines. The dark shading at the catchment outlet reflects an increase in slope of the main stream channel as it falls to meet the Wallagaraugh River.

The final topographic attribute computed by the model is aspect, and its distribution across the Geebung Creek catchment is presented in Figure 7. In this figure aspect is shown in degrees clockwise from north. The

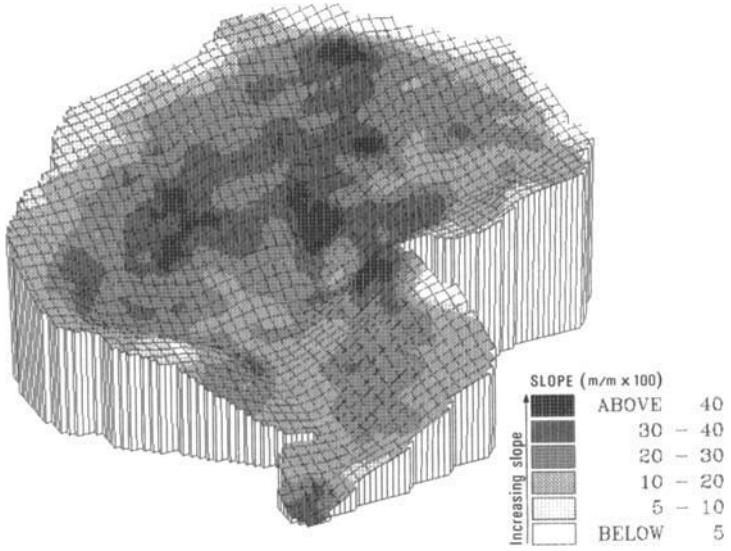

Figure 6. Distribution of slope classes (m/m × 100) computed by the topographic model for the 79·6 ha Geebung Creek catchment

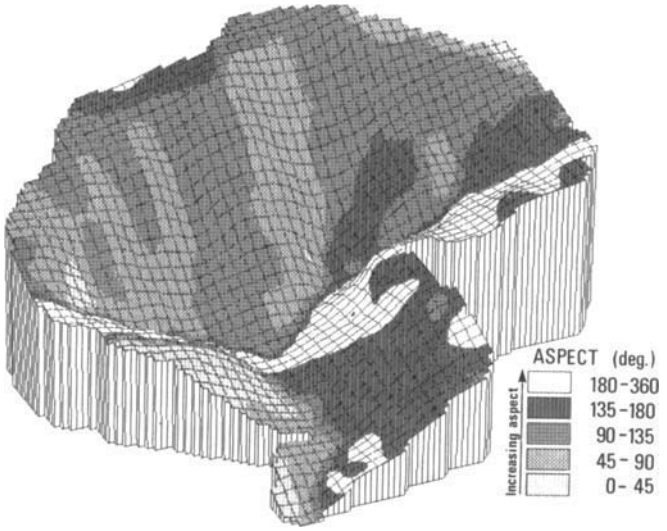

Figure 7. Distribution of aspect classes (angle in degrees, measured clockwise from north) computed by the topographic model for the 79·6 ha Geebung Creek catchment

catchment has a general easterly aspect, with major portions having northeast to east (45°–90°) and east to southeastern (90°–135°) aspects. Only small areas have south to north (180°–360°) aspects, the unshaded areas in Figure 7, but these are mostly hidden in the figure because of the view angle used to present the results. Therefore, large sections of the catchment would receive the morning sun and would be shaded in the late afternoon.

APPLICATIONS OF THE MODEL

Prediction of zones of saturation in a catchment

Many aspects of hydrologic behaviour in small catchments are associated with their saturated source area characteristics. These saturated source areas expand and contract as a direct consequence of the wetting-up and drying-out of the catchment and generate overland flow during rainfall events (Hewlett and Nutter, 1970). This overland flow appears as rapid runoff in the storm hydrograph. The same areas are often the most sensitive to mechanical disturbance because of low soil strength, and are liable to become salinized if solutes present in the seepage water become sufficiently concentrated at the surface. The location and size of these zones is therefore of direct interest for interpreting a range of catchment hydrologic processes, especially in cases where land use or vegetation management could alter the behaviour of these zones.

Beven and Kirkby (1979), O'Loughlin (1981, 1986) and Zaslavsky and Sinai (1981) observed that variations in wetness within a catchment are explicable in terms of the local topography (slope and degree of convergence of the hillslope) and the hydraulic properties of the soil profile (*viz.* the often observed decrease in hydraulic conductivity with depth below the soil surface). Local saturation at any point in a catchment will occur whenever the drainage flux from upslope exceeds the capacity of the soil profile to transmit the flux. O'Loughlin (1981) expressed this criterion as

$$Q_b / Sb \geqslant T \tag{4}$$

where b is the length of the contour element (see Figure 1), Q_b is the local drainage flux across this element, S is the local hillslope gradient (m m^{-1}), and T is the soil transmissivity (the depth integrated saturated hydraulic conductivity). This relationship assumes that lateral drainage takes place over an effectively impermeable layer (relative to the lateral water flux) and that the slope of the land surface approximates the water table gradient. By assuming steady-state drainage conditions, O'Loughlin (1986) recast equation (4) in a form that can

account for variable drainage fluxes and transmissivities over a catchment. This relationship can be written in a dimensionless form as

$$D = \frac{1}{SbL}\left(\frac{\bar{T}}{T}\right)\int\left(\frac{q}{q_0}\right)\mathrm{d}A \geqslant \frac{\bar{T}}{q_0 L} = W \tag{5}$$

where q is the drainage flux per unit area (flux density), $\mathrm{d}A$ is the area contributing to drainage upslope of a contour element of width b, $\bar{T}$ and q_0 are the average catchment transmissivity and drainage flux density, respectively, L is a characteristic length used to make the expression dimensionless (mean hillslope length), D is a drainage index, and W is a wetness index. More detailed descriptions of the derivation of this equation and the assumptions involved are given in O'Loughlin (1986).

The term on the left hand side of equation (5), the drainage index, consists of two dimensionless ratios (q/q_0 and $\bar{T}/T$) and four topographic attributes (S, b, $\mathrm{d}A$, and L), three of which (S, b, and $\mathrm{d}A$) can be calculated throughout a catchment by the topographic model proposed herein. Thus, by combining equation (5) with the topographic model it is possible to calculate drainage indices, and hence identify zones of surface saturation, in complex three-dimensional terrain. The simplest case that can be considered is to assume that the drainage flux density and transmissivity are uniform throughout the catchment (i.e. $q/q_0 = 1$ and $\bar{T}/T = 1$), in which case equation (5) reduces to

$$D = \frac{1}{SbL}\int\mathrm{d}A \geqslant \frac{\bar{T}}{q_0 L} = W \tag{6}$$

so that the drainage index is a function of topographic attributes only. These assumptions are used here simply to demonstrate the application of the method.

The predicted locations and sizes of the zones of surface saturation for the Geebung Creek catchment are presented in Figure 8 as a function of the drainage index, D. Increasingly darker shadings in this figure reflect increasingly wetter zones in the catchment for a given average drainage flux density, q_0. A given location is predicted to be saturated at the soil surface when the drainage index is greater than the value given in Figure 8. Observations on the catchment confirm these general predictions (Moore *et al.*, 1986).

Moore *et al.* (1986) used the predicted wetness indices, together with measured rainfall–runoff data, to estimate the average transmissivity, T, of the Geebung Creek catchment and found good agreement with the

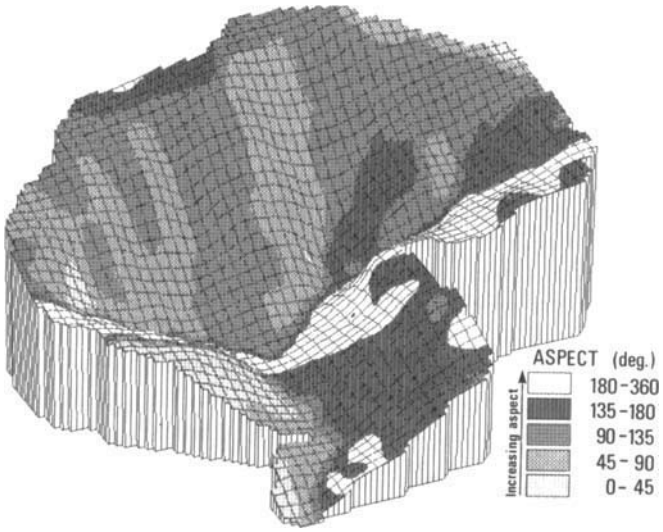

Figure 8. Location and size of zones of saturation on the Geebung Creek catchment predicted as a function of drainage index, D, for the simplest case where the drainage flux density and transmissivity are assumed uniform across the catchment

values computed from measured hydraulic conductivities obtained from soil cores and *in-situ* measurements using a well permeameter (on a grid network across the catchment). Furthermore, they used the calculated wetness index versus per cent saturated source area relationship as the basis for a full dynamic simulation of the rainfall-runoff response of the catchment by assuming successive steady-state conditions. The predicted runoff hydrographs showed excellent agreement with the observed. Detailed descriptions of the techniques used are presented by Moore *et al.* (1986).

These examples illustrate only two ways in which the saturation zone analysis can be used. Further examples include the use of the results by forest managers to optimize the exclusion zones where logging should not be permitted at all and the identification of zones where logging may or may not be permitted, depending on the weather. O'Loughlin (1986) has used the analysis to determine the impacts of selective clearing on the local water balance, and Burch *et al.* (1987) have used it to differentiate between the effects of topography and soil hydraulic properties on runoff generation in cleared and forested catchments.

Prediction of radiation received across a catchment

The effect of topography on the amount of radiation received at the land surface is particularly important in understanding the ecology and the hydrology of catchments. For example, Tajchman and Lacey (1986), using Budyko's (1974) radiation index of dryness (net radiation/latent heat equivalent of precipitation), showed that biomass production on two small catchments was related to aspect, radiation and wetness. Austin *et al.* (1983) have also demonstrated that the distribution of some eucalypt species in southeastern Australia is related to altitude, rainfall, and annual radiation index.

The potential daily solar radiation, R, is a function of the topographic attributes of slope (ε in degrees) and aspect or azimuth (A'—measured clockwise from north), and the solar declination (δ), terrestrial latitude (ϕ), the ratio of the earth–sun distance to its mean (r), the transmission and scattering properties of the atmosphere, and the albedo of the surface (Robinson, 1966; Lee, 1978). A first and simple assumption for demonstration purposes is to neglect atmospheric and surface effects so that diffuse radiation is ignored. The solar declination and the ratio of the earth–sun distance to its mean are essentially constant over a day so that the potential daily solar radiation can be written as

$$R = \frac{24\,Io}{r^2}(\cos\phi'\cos\delta)(\sin\omega t_s' - \omega t_s'\cos\omega t_s') \tag{7}$$

where Io is the solar constant (4·871 MJ m^{-2} h^{-1} or 1·942 Ly min^{-1}), ω is the angular velocity of the earth ($\pi/12$ radians h^{-1}), t_s' is the sunrise–sunset time from solar noon, as seen by the inclined surface. [$\cos\omega t_s' = -\tan\phi'\tan\delta$], $\sin\phi' = \sin\varepsilon\cos A'\cos\phi' + \cos\varepsilon\sin\phi$, and the other symbols are as previously defined. The solar declination ranges from 23·5° at the winter solstice to $-23{\cdot}5°$ at the summer solstice in the southern hemisphere and the ratio of the earth–sun distance to its mean varies in a narrow range from 0·9833 to 1·0167.

The topographic variables required to model the distribution of potential solar radiation, R, across a catchment are local slope and aspect, which are properties of each contour segment. Upslope contributing area is not used in this particular application. The distribution of R across the Geebung Creek catchment was calculated at both the winter and summer solstices ($\delta = 23{\cdot}5°$ and $-23{\cdot}5°$, respectively), representing the minimum and maximum potential daily solar radiation received by the catchment during a year. The results for the winter solstice are presented in Figure 9. The potential daily solar radiation on a horizontal plane (R_h) in the catchment at the winter solstice is 14·1 MJm^{-2} d^{-1} (336 Ly min^{-1}). The R/R_h ratio ranges from a low of 0·25 on sites with southwesterly aspects to a high of about 1·2 on sloping sites with northern and eastern aspects. At the summer solstice R_h is 44·2 MJ m^{-2} d^{-1} (1058 Ly min^{-1}), more than three-fold the winter solstice value, but the R/R_h ratios exhibit less variation, ranging from 0·7 to 1·0.

Austin (personal communication: unpublished manuscript) and Binns (1984) have measured the species composition of the overstorey for the Geebung Creek catchment on 0·1 ha circular plots arranged on a grid pattern. A simplified form of these results is presented in Figure 10, in which the eucalypt species have been divided into four broad groups: (1) *E. sieberi*; (2) *E. agglomerata*; (3) *E. consideniana*; and (4) *E. muellerana*. However, up to one of the other species identified within the parentheses following each group name in the

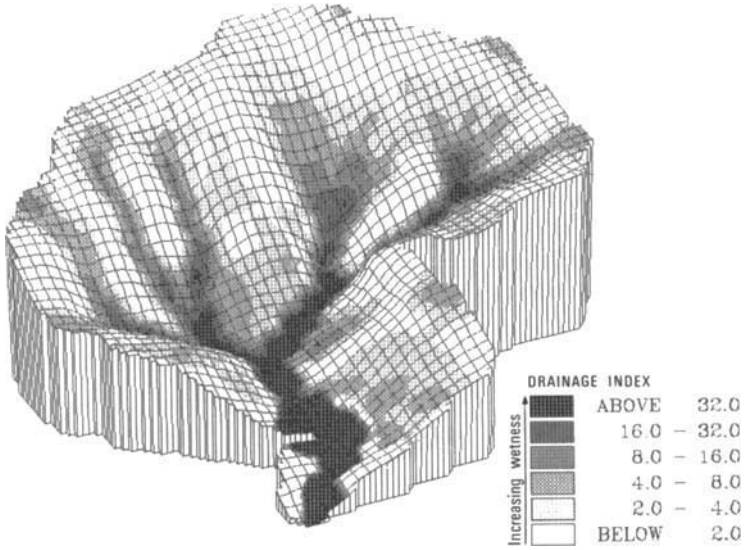

Figure 9. Predicted distribution of potential daily solar radiation, R (MJ m^{-2} d^{-1}), on the Geebung Creek catchment at the winter solstice (June 22)

legend of Figure 10 also has a high probability of being found at the sites indicated on the figure. Species groups 2, 3, and 4 occur predominantly in the wetter and shadier sites, as shown on Figures 8 and 9, respectively, while the group 1 species, the *E. sieberi*, are found mostly in the drier areas receiving higher amounts of radiation. The ridges on the catchment's boundary contain *E. sieberi* almost exclusively. These ridges are both the driest parts of the catchment, as well as the most exposed, receiving the highest potential daily radiation. On the other hand, the authors have observed that none of the eucalypt species in groups 1 to 4 are found in the wettest drainage lines shown in Figure 8 (the areas with a drainage index above 16·0). These observed distributions may also be affected by fire, which undoubtedly plays a part in the relative abundance among eucalypt species in this forest (Bridges, 1983). Both radiation and drainage index variations could be expected to influence the susceptibility of parts of the landscape to fire through their effect on fuel moisture content. These qualitative correlations suggest that linking the distributed results from the saturation-zone

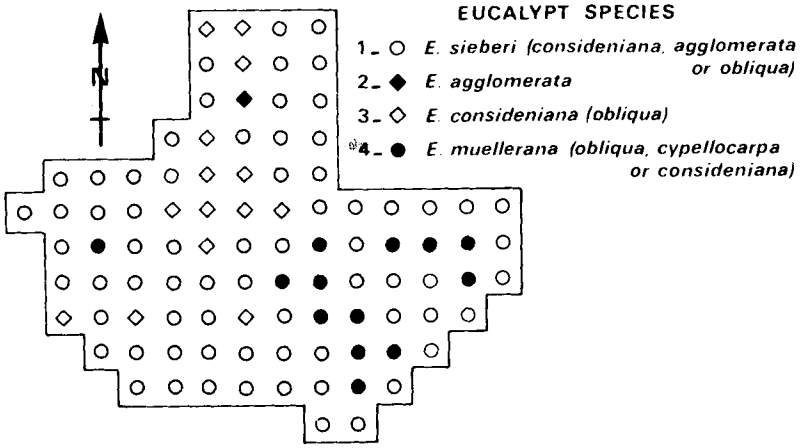

Figure 10. Composition and distribution of eucalypt species in the overstorey of the Geebung Creek catchment measured by Austin (personal communication)

analysis with those from the radiation analysis may prove useful in predicting the distribution and location of different tree and plant species on a catchment.

Prediction of zones of erosion and deposition in a catchment

Estimates of erosion rates, the redistribution of soil within the landscape, and sediment loads in runoff are being increasingly required by land and water resource managers to assess the possible impacts of land use and land management practices on water quality, and land productivity and degradation. Recent emphasis in models for predicting sediment transport have concentrated on detailed representation of the physical processes of soil detachment, entrainment, and transport by rainfall and sheet and rill flow at the plot or hillslope scale (for example, Alonso *et al.*, 1981; Rose *et al.*, 1983; Gilley *et al.*, 1985; and Moore and Burch, 1986a). These models generally idealize the topography as a two-dimensional hillslope and poorly represent overland flow convergence and divergence. Even though they are quite powerful models this is a major deficiency that makes them incapable of accurately predicting erosion and deposition in naturally complex three-dimensional terrain.

However, improved predictions of the sediment fluxes in such complex three-dimensional catchments are possible by combining a soil erosion model with a quantitative three-dimensional description of the hydrology of a catchment, based on a DTM or topographic model. By dividing a catchment into small elements or polygons, the erosion and deposition rates per unit area can be calculated for each element by performing a mass balance of the sediment entering and exiting each element per unit time.

The topographic model described in this paper provides a mechanism for dividing catchments into elements compatible with the physics of overland flow. The topographic variables of local slope and upslope contributing area, calculated by the model, can also be used to determine the discharge per unit width, q, or the average flow velocity, V, at any point in the catchment, thus defining the three-dimensional runoff processes affecting erosion and sediment transport. The simplest case that can be considered is that of steady-state runoff with a uniform rainfall excess throughout the catchment. These assumptions are adopted here for simplicity to illustrate the method. For this assumption $q = rA/b$, where r is the rainfall excess rate, A is the upslope contributing area and b is the width of the contour element, as defined in Figure 1. The flow velocity can then be calculated from the estimates of q, local slope, and surface roughness using Manning's equation or a similar equation (Henderson, 1966), as deemed appropriate. A full dynamic analysis is much more complex.

An example of the potential relative erosion and deposition rates for the Geebung Creek catchment predicted by combining these concepts is presented in Figure 11. In making these predictions it was assumed that sediment transport was transport capacity limited and not detachment limited. The effects of vegetation on erosion and deposition were also neglected. Because of these simplifications the results are presented in terms of potential relative erosion and deposition rates, rather than absolute values, and so only reflect the influence of topography on erosion and deposition. In Figure 11 erosion is negative and deposition is positive.

Yang's (1973) unit stream power equation was chosen as the sediment transport capacity equation in this analysis because it is computationally simple, although any one of several equations that have been proposed in the literature (e.g. Alonso *et al.*, 1981) could be used. This equation can be written as

$$C = \gamma (P - P_{cr})^{\beta} \tag{8}$$

where C is the sediment concentration, P is the unit stream power, P_{cr} is the critical unit stream power at incipient sediment motion, and γ and β are constants that are functions of the median sediment size, the kinematic viscosity of water, and the terminal fall velocity of sediment particles in water. Unit stream power is defined as the time rate of potential energy dissipation per unit weight of water ($= VS$, where V is the flow velocity and S is the slope). Moore and Burch (1986a, 1986b) developed equations for estimating P for sheet and rill flow and demonstrated that equation (8) reliably predicts the sediment transport capacity of shallow sheet and rill flow for medium to coarse textured non-cohesive soils as well as finely aggregated clay soils (Moore and Burch, 1986a). As an example, the equation for shallow sheet flow is

$$P = \frac{q^{0.4}}{n^{0.6}} \left(\frac{\partial y}{\partial s} \right)^{1.3} \tag{9}$$

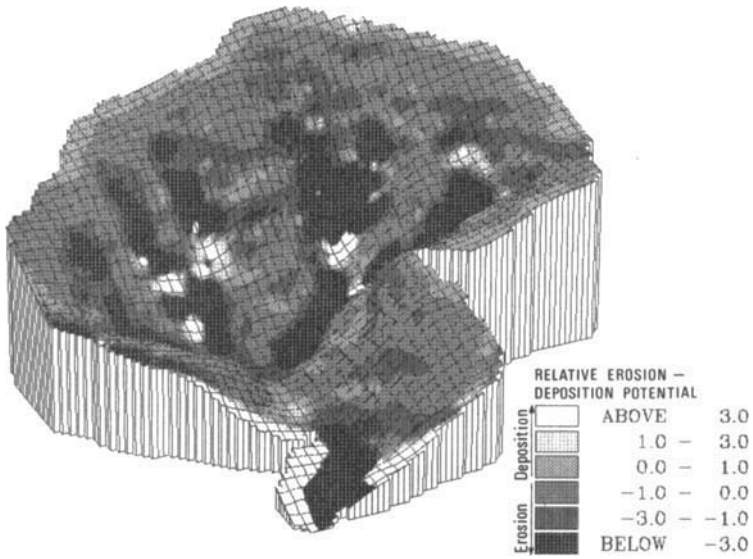

Figure 11. Predicted relative erosion and deposition rates on the Geebung Creek catchment assuming steady-state runoff and a uniform rainfall excess over the catchment. Erosion is negative and deposition is positive.

where n is Manning's roughness coefficient and $\partial y/\partial s$ ($= S$) is the slope orthogonal to the contour. The sediment flux per unit width, Y_b (kg m^{-1} s^{-1}), at any point s is

$$Y_b = \rho q C \tag{10}$$

where ρ is the density of water.

Combining equations 8, 9 and 10 allows the sediment flux per unit width to be calculated at any point in a catchment in terms of the soil properties P_{cr}, n, γ and β (constants) and the hydrologic and topographic variables q and dy/ds, respectively, by making the appropriate assumptions (i.e. steady-state runoff). More detail is given by Moore and Burch (1986b).

As stated previously, most physically based erosion models developed to date represent erosion as a two-dimensional process. However, Moore and Burch (1986b) showed that convergence and divergence of overland flow can significantly affect erosion and deposition. Therefore, the ability to realistically represent the effects of three-dimensional terrain on surface runoff, and hence erosion and deposition, using the outputs from the topographic model provides a significant improvement in our predictive capabilities. The inclusion of three-dimensionality into erosion models also allows such features as the transition of sheet flow to rill flow and the resulting geometry of rill networks to be better represented and predicted. The increase in sediment transport capacity as overland flow is concentrated in rill and channel networks and the influence of surface cover on soil properties and soil detachments are currently recognized as important processes to be represented in predictive models. Erosion and deposition models that realistically represent the three-dimensionality of natural terrain can be used to identify areas of high potential erosion that require special conservation treatment without having to resort to the treatment of entire catchments. This would allow for more efficient and effective use of the limited financial resources available for reducing erosion and sediment discharges from catchments.

CONCLUSIONS

A model for determining the topographic attributes of slope, aspect, and upslope contributing area distributed across three-dimensional terrain is described. The discretization of the terrain produces irregularly shaped polygons based on contour lines and their orthogonals, streamlines, or flow lines. This form of discretization gives the model numerous advantages over existing models, particularly when the model is applied to problems

involving water movement over and through natural three-dimensional terrain. The model was originally developed for hydrological applications and as a result its structure is well suited to representing natural earth surface processes, especially those relating to the hydrology, geomorphology, and sedimentology of landscapes and the physiology of native vegetation. The algorithms used in the model are described according to the two core computer programs that progressively analyse input data that are usually in the form of a digitized topographic map.

Topographic, geomorphic, soil, vegetative, and hydrologic attributes of a small catchment in southeastern Australia are used to demonstrate three applications of the model. In the first application the topographic attributes calculated by the model are used to predict the natural occurrence of seepage or saturation zones within the catchment as an aid in the interpretation of its hydrological behaviour. Secondly, the computed topographic attributes are used to predict the distribution of potential daily solar radiation across the catchment to help interpret the distribution and species composition of tree associations or groupings previously surveyed within the catchment. Finally, the potential relative erosion and deposition rates within the catchment are estimated by combining a sediment transport function with procedures for simulating the hydrology of three-dimensional land surfaces using the calculated topographic attributes. These applications of the model are introduced to demonstrate its versatility and by no means exhaust the possibilities for other applications.

ACKNOWLEDGEMENTS

The authors wish to thank Dr. Mike Hutchinson, CSIRO Division of Water and Land Resources for reviewing an early draft of this paper and for his many comments and suggestions during the course of the study. This work was partially supported by a grant (Project 85/131) from the Australian Water Research Advisory Council.

REFERENCES

Ahnert, F. 1976. 'Brief description of a comprehensive three-dimensional process-response model of landform development', *Zeitschrift für Geomorpholog, N. F., Supplement*, **25**, 29–49.

Alonso, C. V., Neibling, W. H., and Foster, G. R. 1981. 'Estimating sediment transport capacity in watershed modelling', *Transactions of American Society of Agricultural Engineers*, **24**, 1211–1220, 1226.

Armstrong, A. 1976. 'A three-dimensional simulation of slope forms', *Zeitschrift für Geomorpholog, N.F., Supplement*, **25**, 20–28.

Austin, M. P., Cunningham, R. B., and Good, R. B. 1983. 'Altitudinal distribution of several eucalypt species in relation to other environmental factors in southern New South Wales', *Australian Journal of Ecology*, **8**, 169–180.

Band, L. E. 1986. 'Topographic partitioning of waterhseds with digital elevation models', *Water Resources Research*, **22**, 15–24.

Beasley, D. B., Huggins, L. F., and Monke, E. J. 1980. 'ANSWERS: a model for watershed planning', *Transactions of American Society of Agricultural Engineers*, **23**, 938–944.

Beven, K. and Kirkby, M. J. 1979. 'A physically based variable contributing area model of basin hydrology', *Hydrological Sciences Bulletin*, **24**, 43–69.

Binns, D. 1984. 'Vegetation studies', in Eden Catchment Project, 1984 Review, *Forestry Commission of N.S.W., Miscellaneous Paper*, 16–34.

Bridges, R. G. 1983. 'Integrated logging and regeneration in the silvertop ash–stringybark forests of the Eden region', *Forestry Commission of N.S.W., Research Paper No. 2.*

Budyko, M. I. 1974. *Climate and Life*, Academic Press, New York, 508 pp.

Burch, G. J., Bath, R. K., Moore, I. D., and O'Loughlin, E. M. 1987. 'Comparative hydrologic behaviour of forested and cleared catchments in southeastern Australia', *Journal of Hydrology*, **90**, 19–42.

Clerici, D. 1980. 'A method for drawing slope maps by automatic data acquisition and processing', *Computers and Geosciences*, **6**, 289–297.

Gilley, J. E., Woolhiser, D. A., and McWhorter, D. B. 1985. 'Interill soil erosion—Part 1: development of model equations', *Transactions of American Society of Agricultural Engineers*, **28**, 147–153, 159.

Hall, J. K. 1975. 'PTLOC—A FORTRAN subroutine for determining the position of a point relative to a closed boundary', *Mathematical Geology*, **7**, 75–79.

Heerdegen, R. G. and Beran, M. A. 1982. 'Quantifying source areas through land surface curvature and shape', *J. Hydrol.*, **57**, 359–373.

Henderson, F. M. 1966. *Open Channel Flow*, Macmillan, New York, 90–101.

Hewlett, J. D. and Nutter, W. L. 1970. *The varying source area of streamflow from upland basins*, paper presented at the Symp. on Interdisciplinary Aspects of Watershed Management, Montana State Univ., Bozeman, Mont.

Hirano, M. 1976. 'Mathematical model and concept of equilibrium in connection with slope shear ratio', *Zeitschrift für Geomorpholog, N.F., Supplement*, **25**, 50–71.

Hutchinson, M. F. 1981. 'MAPROJ—a computer map projection system', *CSIRO Division of Land Use Research, Tech. Paper No. 39.*

Hutchinson, M. F. 1984. 'A summary of some surface fitting and contouring programs for noisy data', *CSIRO Div. Maths. and Stats. Consulting Report 84/6.*

Lee, R. 1978. *Forest Microclimatology*, Columbia Univ. Press, New York, 33–84.

Linsley Jr., R. K., Kohler, M. A., and Paulus, J. L. H. 1949. *Applied Hydrology*, McGraw-Hill, New York, 252 pp.

Mackay, S. M. and Cornish, P. M. 1982. 'Effect of wildfire and logging on the hydrology of small catchments near Eden, N.S.W.', *The First National Symposium on Forest Hydrology, Inst. Eng., Aust. Natl. Conf. Publ. No. 82/6*, 111–117.

Mark, D. M. 1978. 'Concepts of "data structure" for digital terrain models', *Proc. Digital Terrain Models (DTM) Symposium, St. Louis, Missouri, May 1978*, 24–31.

Moore, I. D. and Burch, G. J. 1986a. 'Sediment transport capacity of sheet and rill flow: Application of unit stream power theory'. *Water Resources Research*, **22,** 8, 1350–1360.

Moore, I. D. and Burch, G. J. 1986b. 'Modelling erosion and deposition: topographic effects', *Transactions of American Society of Agricultural Engineers*, **29,** 6, 1624–1630, 1640.

Moore, I. D., Mackay, S. M., Wallbrink, P. J., Burch, G. J., and O'Loughlin, E. M. 1986. 'Hydrologic characteristics and modelling of a small forested catchment in southeastern New South Wales. Pre-logging condition', *Journal of Hydrology*, **83,** 307–335.

Mulla, D. J. 1986. 'Distribution of slope steepness in the Palouse region of Washington'. *Soil Sci. Soc. Am. J.*, **50,** 6, 1401–1406.

O'Callaghan, J. F. and Mark, D. M. 1984. 'The extraction of drainage networks from digital elevation data', *Computer Vision Graphics and Image Processing*, **28,** 323–344.

O'Loughlin, E. M. 1981. 'Saturation regions in catchments and their relations to soil and topographic properties', *Journal of Hydrology*, **53,** 229–246.

O'Loughlin, E. M. 1986. 'Prediction of surface saturation zones in natural catchments by topographic analysis', *Water Resources Research*, **22,** 5, 794–804.

O'Loughlin, E. M. in press. 'WETZONE: A computer system for topographic analysis of landscapes for hydrologic applications', *CSIRO Div. Water and Land Resour. Tech. Memo.*

Robinson, N. 1966. *Solar Radiation*, Elsevier, New York, 29–160.

Rose, C. W., Williams, J. R., Sander, G. C., and Barry, D. A. 1983. 'A mathematical model of soil erosion and deposition processes: I. Theory for a plane land element', *Soil Science Society of America Journal*, **47,** 5, 991–995.

Sharpnack, D. A. and Akin, G. 1969. 'An algorithm for computing slope and aspect from elevations', *Photogramm. Eng.*, **35,** 247–268.

Tajchman, S. J. and Lacey, C. J. 1986. 'Bioclimatic factors in forest site potential'. *Forest Ecology and Management*, **14,** 211–218.

Travis, M. R., Elsnes, G. H., Iverson, W. D., and Johnson, C. G. 1975. 'VIEWIT: Computation of seen areas, slope and aspect for land use planning', *Pacific Southwest Forest and Range Experiment Station, USDA For. Ser. Gen. Tech. Rep.*, **PSW-11,** 1–70.

Yang, C. T. 1973. 'Incipient motion and sediment transport', *Proceedings of the American Society of Civil Engineering, Journal of Hydraulics Division*, 99, **HY10,** 1679–1704.

Zaslavsky, D. and Sinai, G. 1981. 'Surface hydrology: I. Explanation of phenomena, II. Distribution of raindrops, III. Causes of lateral flow, IV. Flow in sloping layered soil, V. In-surface transient flow', *Proceedings of the American Society of Civil Engineering, Journal of Hydraulics Division*, **HY1,** 1–93.